EUROPEAN ORGANIZATION FOR NUCLEAR RESEARCH

CERN–EP/98–115

1st July 1998

Measurement of $|V_{cs}|$ using W decays at LEP2

DELPHI Collaboration

Abstract

Decays of $W^{\pm}$ bosons, produced at LEP2, have been used to measure the $|V_{cs}|$ element of the Cabibbo-Kobayashi-Maskawa matrix. Values for $|V_{cs}|$ were extracted both from the measured hadronic branching ratio of $W^{\pm}$ decays and by tagging the flavour of hadronic jets produced in $W^{\pm}$ decays. Applying the two methods to the data collected during 1996 at energies of 161 and 172 GeV, DELPHI obtains $|V_{cs}| = 0.91\,^{+0.15}_{-0.14}(stat) \pm 0.05(syst)$.

(Accepted by Phys. Lett. B)

P.Abreu[21], W.Adam[50], T.Adye[36], P.Adzic[11], I.Ajinenko[42], G.D.Alekseev[16], R.Alemany[49], P.P.Allport[22], S.Almehed[24], U.Amaldi[9], S.Amato[47], E.G.Anassontzis[3], P.Andersson[44], A.Andreazza[9], S.Andringa[21], P.Antilogus[25], W-D.Apel[17], Y.Arnoud[14], B.Åsman[44], J-E.Augustin[25], A.Augustinus[9], P.Baillon[9], P.Bambade[19], F.Barao[21], G.Barbiellini[46], R.Barbier[25], D.Y.Bardin[16], G.Barker[9], A.Baroncelli[38], M.Battaglia[15], M.Baubillier[23], K-H.Becks[52], M.Begalli[6], P.Beilliere[8], Yu.Belokopytov[9,53], K.Belous[42], A.C.Benvenuti[5], C.Berat[14], M.Berggren[25], D.Bertini[25], D.Bertrand[2], M.Besancon[39], F.Bianchi[45], M.Bigi[45], M.S.Bilenky[16], M-A.Bizouard[19], D.Bloch[10], H.M.Blom[30], M.Bonesini[27], W.Bonivento[27], M.Boonekamp[39], P.S.L.Booth[22], A.W.Borgland[4], G.Borisov[19], C.Bosio[41], O.Botner[48], E.Boudinov[30], B.Bouquet[19], C.Bourdarios[19], T.J.V.Bowcock[22], I.Boyko[16], I.Bozovic[11], M.Bozzo[13], P.Branchini[38], T.Brenke[52], R.A.Brenner[48], P.Bruckman[18], J-M.Brunet[8], L.Bugge[32], T.Buran[32], T.Burgsmueller[52], P.Buschmann[52], S.Cabrera[49], M.Caccia[27], M.Calvi[27], A.J.Camacho Rozas[40], T.Camporesi[9], V.Canale[37], F.Carena[9], L.Carroll[22], C.Caso[13], M.V.Castillo Gimenez[49], A.Cattai[9], F.R.Cavallo[5], Ch.Cerruti[10], V.Chabaud[9], M.Chapkin[42], Ph.Charpentier[9], L.Chaussard[25], P.Checchia[35], G.A.Chelkov[16], M.Chen[2], R.Chierici[45], P.Chliapnikov[42], P.Chochula[7], V.Chorowicz[25], J.Chudoba[29], P.Collins[9], M.Colomer[49], R.Contri[13], E.Cortina[49], G.Cosme[19], F.Cossutti[39], J-H.Cowell[22], H.B.Crawley[1], D.Crennell[36], G.Crosetti[13], J.Cuevas Maestro[33], S.Czellar[15], G.Damgaard[28], M.Davenport[9], W.Da Silva[23], A.Deghorain[2], G.Della Ricca[46], P.Delpierre[26], N.Demaria[9], A.De Angelis[9], W.De Boer[17], S.De Brabandere[2], C.De Clercq[2], B.De Lotto[46], A.De Min[35], L.De Paula[47], H.Dijkstra[9], L.Di Ciaccio[37], A.Di Diodato[37], A.Djannati[8], J.Dolbeau[8], K.Doroba[51], M.Dracos[10], J.Drees[52], K.-A.Drees[52], M.Dris[31], A.Duperrin[25], J-D.Durand[25,9], R.Ehret[17], G.Eigen[4], T.Ekelof[48], G.Ekspong[44], M.Ellert[48], M.Elsing[9], J-P.Engel[10], B.Erzen[43], M.Espirito Santo[21], E.Falk[24], G.Fanourakis[11], D.Fassouliotis[11], J.Fayot[23], M.Feindt[17], A.Fenyuk[42], P.Ferrari[27], A.Ferrer[49], E.Ferrer-Ribas[19], S.Fichet[23], A.Firestone[1], P.-A.Fischer[9], U.Flagmeyer[52], H.Foeth[9], E.Fokitis[31], F.Fontanelli[13], B.Franek[36], A.G.Frodesen[4], R.Fruhwirth[50], F.Fulda-Quenzer[19], J.Fuster[49], A.Galloni[22], D.Gamba[45], S.Gamblin[19], M.Gandelman[47], C.Garcia[49], J.Garcia[40], C.Gaspar[9], M.Gaspar[47], U.Gasparini[35], Ph.Gavillet[9], E.N.Gazis[31], D.Gele[10], J-P.Gerber[10], N.Ghodbane[25], I.Gil[49], F.Glege[52], R.Gokieli[51], B.Golob[43], P.Goncalves[21], I.Gonzalez Caballero[40], G.Gopal[36], L.Gorn[1,54], M.Gorski[51], Yu.Gouz[42], V.Gracco[13], J.Grahl[1], E.Graziani[38], C.Green[22], A.Grefrath[52], P.Gris[39], K.Grzelak[51], M.Gunther[48], J.Guy[36], F.Hahn[9], S.Hahn[52], S.Haider[9], A.Hallgren[48], K.Hamacher[52], F.J.Harris[34], V.Hedberg[24], S.Heising[17], J.J.Hernandez[49], P.Herquet[2], H.Herr[9], T.L.Hessing[34], J.-M.Heuser[52], E.Higon[49], S-O.Holmgren[44], P.J.Holt[34], D.Holthuizen[30], S.Hoorelbeke[2], M.Houlden[22], J.Hrubec[50], K.Huet[2], K.Hultqvist[44], J.N.Jackson[22], R.Jacobsson[9], P.Jalocha[9], R.Janik[7], Ch.Jarlskog[24], G.Jarlskog[24], P.Jarry[39], B.Jean-Marie[19], E.K.Johansson[44], P.Jonsson[24], C.Joram[9], P.Juillot[10], F.Kapusta[23], K.Karafasoulis[11], S.Katsanevas[25], E.C.Katsoufis[31], R.Keranen[17], B.A.Khomenko[16], N.N.Khovanski[16], A.Kiiskinen[15], B.King[22], N.J.Kjaer[30], O.Klapp[52], H.Klein[9], P.Kluit[30], D.Knoblauch[17], P.Kokkinias[11], M.Koratzinos[9], C.Kourkoumelis[3], O.Kouznetsov[16], M.Krammer[50], C.Kreuter[9], E.Kriznic[43], J.Krstic[11], Z.Krumstein[16], P.Kubinec[7], W.Kucewicz[18], K.Kurvinen[15], J.W.Lamsa[1], D.W.Lane[1], P.Langefeld[52], V.Lapin[42], J-P.Laugier[39], R.Lauhakangas[15], F.Ledroit[14], V.Lefebure[2], L.Leinonen[44], A.Leisos[11], R.Leitner[29], J.Lemonne[2], G.Lenzen[52], V.Lepeltier[19], T.Lesiak[18], M.Lethuillier[39], J.Libby[34], D.Liko[9], A.Lipniacka[44], I.Lippi[35], B.Loerstad[24], J.G.Loken[34], J.H.Lopes[47], J.M.Lopez[40], R.Lopez-Fernandez[14], D.Loukas[11], P.Lutz[39], L.Lyons[34], J.MacNaughton[50], J.R.Mahon[6], A.Maio[21], A.Malek[52], T.G.M.Malmgren[44], V.Malychev[16], F.Mandl[50], J.Marco[40], R.Marco[40], B.Marechal[47], M.Margoni[35], J-C.Marin[9], C.Mariotti[9], A.Markou[11], C.Martinez-Rivero[19], F.Martinez-Vidal[49], S.Marti i Garcia[22], N.Mastroyiannopoulos[11], F.Matorras[40], C.Matteuzzi[27], G.Matthiae[37], J.Mazik[29], F.Mazzucato[35], M.Mazzucato[35], M.Mc Cubbin[22], R.Mc Kay[1], R.Mc Nulty[9], G.Mc Pherson[22], C.Meroni[27], A.Miagkov[42], E.Migliore[45], L.Mirabito[25], W.A.Mitaroff[50], U.Mjoernmark[24], T.Moa[44], R.Moeller[28], K.Moenig[9], M.R.Monge[13], X.Moreau[23], P.Morettini[13], G.Morton[34], K.Muenich[52], M.Mulders[30], C.Mulet-Marquis[14], R.Muresan[24], W.J.Murray[36], B.Muryn[14,18], G.Myatt[34], T.Myklebust[32], F.Naraghi[14], F.L.Navarria[5], S.Navas[49], K.Nawrocki[51], P.Negri[27], S.Nemecek[12], N.Neufeld[9], W.Neumann[52], N.Neumeister[50], R.Nicolaidou[14], B.S.Nielsen[28], V.Nikolaenko[10], M.Nikolenko[10,16], V.Nomokonov[15], A.Normand[22], A.Nygren[24], V.Obraztsov[42], A.G.Olshevski[16], A.Onofre[21], R.Orava[15], G.Orazi[10], K.Osterberg[15], A.Ouraou[39], M.Paganoni[27], S.Paiano[5], R.Pain[23], R.Paiva[21], J.Palacios[34], H.Palka[18], Th.D.Papadopoulou[31], K.Papageorgiou[11], L.Pape[9], C.Parkes[34], F.Parodi[13], U.Parzefall[22], A.Passeri[38], M.Pegoraro[35], L.Peralta[21], M.Pernicka[50], A.Perrotta[5], C.Petridou[46], A.Petrolini[13], H.T.Phillips[36], G.Piana[13], F.Pierre[39], M.Pimenta[21], E.Piotto[27], T.Podobnik[43], M.E.Pol[6], G.Polok[18], P.Poropat[46], V.Pozdniakov[16], P.Privitera[37], N.Pukhaeva[16], A.Pullia[27], D.Radojicic[34], S.Ragazzi[27], H.Rahmani[31], D.Rakoczy[50], P.N.Ratoff[20], A.L.Read[32], P.Rebecchi[9], N.G.Redaelli[27], M.Regler[50], D.Reid[9], R.Reinhardt[52], P.B.Renton[34], L.K.Resvanis[3], F.Richard[19], J.Ridky[12], G.Rinaudo[45], O.Rohne[32], A.Romero[45], P.Ronchese[35], E.I.Rosenberg[1], P.Rosinsky[7], P.Roudeau[19], T.Rovelli[5], V.Ruhlmann-Kleider[39], A.Ruiz[40], H.Saarikko[15], Y.Sacquin[39], A.Sadovsky[16], G.Sajot[14], J.Salt[49], D.Sampsonidis[11], M.Sannino[13], H.Schneider[17], Ph.Schwemling[23], U.Schwickerath[17], M.A.E.Schyns[52], F.Scuri[46], P.Seager[20], Y.Sedykh[16], A.M.Segar[34], R.Sekulin[36], R.C.Shellard[6], A.Sheridan[22], R.Silvestre[39], L.Simard[39], F.Simonetto[35], A.N.Sisakian[16], T.B.Skaali[32], G.Smadja[25], N.Smirnov[42], O.Smirnova[24], G.R.Smith[36], O.Solovianov[42], A.Sopczak[17], R.Sosnowski[51], T.Spassov[21], E.Spiriti[38], P.Sponholz[52], S.Squarcia[13], D.Stampfer[50], C.Stanescu[38], S.Stanic[43], S.Stapnes[32], K.Stevenson[34], A.Stocchi[19], J.Strauss[50], R.Strub[10], B.Stugu[4], M.Szczekowski[51], M.Szeptycka[51], T.Tabarelli[27], F.Tegenfeldt[48], F.Terranova[27], J.Thomas[34], A.Tilquin[26], J.Timmermans[30], L.G.Tkatchev[16], T.Todorov[10], S.Todorova[10], D.Z.Toet[30], A.Tomaradze[2], B.Tome[21], A.Tonazzo[27], L.Tortora[38], G.Transtromer[24],

D.Treille[9], G.Tristram[8], C.Troncon[27], A.Tsirou[9], M-L.Turluer[39], I.A.Tyapkin[16], S.Tzamarias[11], B.Ueberschaer[52], O.Ullaland[9], V.Uvarov[42], G.Valenti[5], E.Vallazza[46], G.W.Van Apeldoorn[30], P.Van Dam[30], J.Van Eldik[30], A.Van Lysebetten[2], I.Van Vulpen[30], N.Vassilopoulos[34], G.Vegni[27], L.Ventura[35], W.Venus[36], F.Verbeure[2], M.Verlato[35], L.S.Vertogradov[16], V.Verzi[37], D.Vilanova[39], L.Vitale[46], E.Vlasov[42], A.S.Vodopyanov[16], G.Voulgaris[3], V.Vrba[12], H.Wahlen[52], C.Walck[44], C.Weiser[17], D.Wicke[52], J.H.Wickens[2], G.R.Wilkinson[9], M.Winter[10], M.Witek[18], G.Wolf[9], J.Yi[1], O.Yushchenko[42], A.Zaitsev[42], A.Zalewska[18], P.Zalewski[51], D.Zavrtanik[43], E.Zevgolatakos[11], N.I.Zimin[16,24], G.C.Zucchelli[44], G.Zumerle[35]

[1] Department of Physics and Astronomy, Iowa State University, Ames IA 50011-3160, USA
[2] Physics Department, Univ. Instelling Antwerpen, Universiteitsplein 1, BE-2610 Wilrijk, Belgium
and IIHE, ULB-VUB, Pleinlaan 2, BE-1050 Brussels, Belgium
and Faculté des Sciences, Univ. de l'Etat Mons, Av. Maistriau 19, BE-7000 Mons, Belgium
[3] Physics Laboratory, University of Athens, Solonos Str. 104, GR-10680 Athens, Greece
[4] Department of Physics, University of Bergen, Allégaten 55, NO-5007 Bergen, Norway
[5] Dipartimento di Fisica, Università di Bologna and INFN, Via Irnerio 46, IT-40126 Bologna, Italy
[6] Centro Brasileiro de Pesquisas Físicas, rua Xavier Sigaud 150, BR-22290 Rio de Janeiro, Brazil
and Depto. de Física, Pont. Univ. Católica, C.P. 38071 BR-22453 Rio de Janeiro, Brazil
and Inst. de Física, Univ. Estadual do Rio de Janeiro, rua São Francisco Xavier 524, Rio de Janeiro, Brazil
[7] Comenius University, Faculty of Mathematics and Physics, Mlynska Dolina, SK-84215 Bratislava, Slovakia
[8] Collège de France, Lab. de Physique Corpusculaire, IN2P3-CNRS, FR-75231 Paris Cedex 05, France
[9] CERN, CH-1211 Geneva 23, Switzerland
[10] Institut de Recherches Subatomiques, IN2P3 - CNRS/ULP - BP20, FR-67037 Strasbourg Cedex, France
[11] Institute of Nuclear Physics, N.C.S.R. Demokritos, P.O. Box 60228, GR-15310 Athens, Greece
[12] FZU, Inst. of Phys. of the C.A.S. High Energy Physics Division, Na Slovance 2, CZ-180 40, Praha 8, Czech Republic
[13] Dipartimento di Fisica, Università di Genova and INFN, Via Dodecaneso 33, IT-16146 Genova, Italy
[14] Institut des Sciences Nucléaires, IN2P3-CNRS, Université de Grenoble 1, FR-38026 Grenoble Cedex, France
[15] Helsinki Institute of Physics, HIP, P.O. Box 9, FI-00014 Helsinki, Finland
[16] Joint Institute for Nuclear Research, Dubna, Head Post Office, P.O. Box 79, RU-101 000 Moscow, Russian Federation
[17] Institut für Experimentelle Kernphysik, Universität Karlsruhe, Postfach 6980, DE-76128 Karlsruhe, Germany
[18] Institute of Nuclear Physics and University of Mining and Metalurgy, Ul. Kawiory 26a, PL-30055 Krakow, Poland
[19] Université de Paris-Sud, Lab. de l'Accélérateur Linéaire, IN2P3-CNRS, Bât. 200, FR-91405 Orsay Cedex, France
[20] School of Physics and Chemistry, University of Lancaster, Lancaster LA1 4YB, UK
[21] LIP, IST, FCUL - Av. Elias Garcia, 14-1°, PT-1000 Lisboa Codex, Portugal
[22] Department of Physics, University of Liverpool, P.O. Box 147, Liverpool L69 3BX, UK
[23] LPNHE, IN2P3-CNRS, Univ. Paris VI et VII, Tour 33 (RdC), 4 place Jussieu, FR-75252 Paris Cedex 05, France
[24] Department of Physics, University of Lund, Sölvegatan 14, SE-223 63 Lund, Sweden
[25] Université Claude Bernard de Lyon, IPNL, IN2P3-CNRS, FR-69622 Villeurbanne Cedex, France
[26] Univ. d'Aix - Marseille II - CPP, IN2P3-CNRS, FR-13288 Marseille Cedex 09, France
[27] Dipartimento di Fisica, Università di Milano and INFN, Via Celoria 16, IT-20133 Milan, Italy
[28] Niels Bohr Institute, Blegdamsvej 17, DK-2100 Copenhagen Ø, Denmark
[29] NC, Nuclear Centre of MFF, Charles University, Areal MFF, V Holesovickach 2, CZ-180 00, Praha 8, Czech Republic
[30] NIKHEF, Postbus 41882, NL-1009 DB Amsterdam, The Netherlands
[31] National Technical University, Physics Department, Zografou Campus, GR-15773 Athens, Greece
[32] Physics Department, University of Oslo, Blindern, NO-1000 Oslo 3, Norway
[33] Dpto. Fisica, Univ. Oviedo, Avda. Calvo Sotelo s/n, ES-33007 Oviedo, Spain
[34] Department of Physics, University of Oxford, Keble Road, Oxford OX1 3RH, UK
[35] Dipartimento di Fisica, Università di Padova and INFN, Via Marzolo 8, IT-35131 Padua, Italy
[36] Rutherford Appleton Laboratory, Chilton, Didcot OX11 OQX, UK
[37] Dipartimento di Fisica, Università di Roma II and INFN, Tor Vergata, IT-00173 Rome, Italy
[38] Dipartimento di Fisica, Università di Roma III and INFN, Via della Vasca Navale 84, IT-00146 Rome, Italy
[39] DAPNIA/Service de Physique des Particules, CEA-Saclay, FR-91191 Gif-sur-Yvette Cedex, France
[40] Instituto de Fisica de Cantabria (CSIC-UC), Avda. los Castros s/n, ES-39006 Santander, Spain
[41] Dipartimento di Fisica, Università degli Studi di Roma La Sapienza, Piazzale Aldo Moro 2, IT-00185 Rome, Italy
[42] Inst. for High Energy Physics, Serpukov P.O. Box 35, Protvino, (Moscow Region), Russian Federation
[43] J. Stefan Institute, Jamova 39, SI-1000 Ljubljana, Slovenia and Department of Astroparticle Physics, School of Environmental Sciences, Kostanjeviska 16a, Nova Gorica, SI-5000 Slovenia,
and Department of Physics, University of Ljubljana, SI-1000 Ljubljana, Slovenia
[44] Fysikum, Stockholm University, Box 6730, SE-113 85 Stockholm, Sweden
[45] Dipartimento di Fisica Sperimentale, Università di Torino and INFN, Via P. Giuria 1, IT-10125 Turin, Italy
[46] Dipartimento di Fisica, Università di Trieste and INFN, Via A. Valerio 2, IT-34127 Trieste, Italy
and Istituto di Fisica, Università di Udine, IT-33100 Udine, Italy
[47] Univ. Federal do Rio de Janeiro, C.P. 68528 Cidade Univ., Ilha do Fundão BR-21945-970 Rio de Janeiro, Brazil
[48] Department of Radiation Sciences, University of Uppsala, P.O. Box 535, SE-751 21 Uppsala, Sweden
[49] IFIC, Valencia-CSIC, and D.F.A.M.N., U. de Valencia, Avda. Dr. Moliner 50, ES-46100 Burjassot (Valencia), Spain
[50] Institut für Hochenergiephysik, Österr. Akad. d. Wissensch., Nikolsdorfergasse 18, AT-1050 Vienna, Austria
[51] Inst. Nuclear Studies and University of Warsaw, Ul. Hoza 69, PL-00681 Warsaw, Poland
[52] Fachbereich Physik, University of Wuppertal, Postfach 100 127, DE-42097 Wuppertal, Germany
[53] On leave of absence from IHEP Serpukhov
[54] Now at University of Florida

1 Introduction

In the Standard Model with $SU(2) \times U(1)$ as the gauge group of the electroweak interaction, the quark mass eigenstates are not the same as the weak eigenstates. For the six quarks, the two bases are related by the unitary 3×3 Cabibbo-Kobayashi-Maskawa (CKM) matrix [1–3]. Apart from the matrix elements describing the decays of the heavy t quark, the value of the element relating the quarks of the second generation is known with the poorest precision. The uncertainty of $\pm 18\%$ on $|V_{cs}|$, determined in semileptonic decays of D mesons [3], is dominated by the poorly known hadronic form-factors.

Hadronic decays of charged weak bosons, $W^{\pm}$, produced in e^+e^- interactions at the upgraded LEP2 collider, offer an alternative measurement. In the decays $W^{\pm} \to q_1\overline{q}_2$, the coupling of the $W^{\pm}$ to the quarks q_1 and $\overline{q}_2$ is proportional to the appropriate CKM matrix element $V_{q_1q_2}$. Therefore the value of $|V_{cs}|$ can be extracted from the measured rate of $W^+ \to c\overline{s}$ decays[1].

The value of $|V_{cs}|$ affects the ratio of hadronic $W^{\pm}$ decays to leptonic $W^{\pm}$ decays. A value for $|V_{cs}|$ can therefore be obtained by measuring the hadronic branching ratio of the $W^{\pm}$ and by setting all other parameters of the Standard Model to their measured values.

Additional information can be obtained by tagging the flavours of the jets produced in hadronic $W^{\pm}$ decays. The flavours of primary quarks from $W^{\pm}$ decays are heavily veiled in the process of hadronization. Nevertheless, some of the properties of the resulting hadronic jets can still reveal information about their origins. Tagging the flavours of jets in the DELPHI detector is based on measured impact parameters and particle identification.

The results of the two methods are independent and can therefore be combined to give a more precise measurement.

2 The DELPHI detector

A detailed description of the DELPHI apparatus and its performance can be found elsewhere [4,5]. Here we briefly review the most important properties of the detector relevant to these measurements.

The detector consists of a cylindrical part, covering the barrel region, and two end-caps. A large superconducting solenoid provides a magnetic field of 1.2 T inside the central tracking volume. The tracking part of the detector consists of the Vertex Detector (VD), Inner Detector (ID), Time Projection Chamber (TPC) and Outer Detector (OD) in the barrel region, and forward chambers. The VD is composed of three cylindrical layers of silicon microstrip modules, each covering the polar angle interval between 25° and 155°, and of additional microstrip and pixel silicon detectors covering the end-cap region [6]. The resolution of particle impact parameters achieved by the VD is a function of particle momentum p and polar angle θ. For the barrel part it can be parameterized by the function $28\mu m \oplus 71\mu m/(p[GeV]\sin^{\frac{3}{2}}\theta)$ in the $R\phi$ plane and by $39\mu m \oplus 75\mu m/(p[GeV]\sin^{\frac{5}{2}}\theta)$ in Rz. The ID and the TPC cover the polar angles between 20° and 160° while the OD improves the momentum resolution for particles with $42° \leq \theta \leq 138°$. The combined performance of the tracking detectors results in a relative momentum resolution better than 1% for charged particles with momenta around 1 GeV/c in hadronic jets emitted perpendicular to the beam axis.

The barrel and forward electromagnetic calorimeters are used to measure the electromagnetic energy deposited by particles with $43° \leq \theta \leq 137°$ and $10° \leq \theta \leq 36.5°$ and

[1] Throughout the paper references to a specific charge state imply the charge conjugate state as well, unless explicitly stated otherwise.

$143.5° \leq \theta \leq 170°$. The small angle tile calorimeter (STIC) [7] covers the two regions between 29 and 185 mrad with respect to the beam line in the forward and backward hemispheres. It measures the electromagnetic energy deposited by particles flying at small angles to the beam pipe, such as Bhabha electrons or photons radiated from the initial state electrons and positrons. The hadron calorimeter measures the energy of hadrons with polar angle between 10° and 170°.

Electron candidates are identified by the characteristic energy deposition in the electromagnetic calorimeters. The efficiency for the identification of electrons with momenta greater than 3 GeV/c varies between 45% and 80% [5], depending on the required purity of the sample. Muons are recognized by the associated hits in the muon chambers surrounding the hadron calorimeter, and by an energy deposition in the hadronic calorimeter compatible with the passage of a minimum ionizing particle. The efficiency for muon identification, obtained from the simulation and from measured $Z^0 \to \mu^+\mu^-$ decays, varies between 76% and 96% [5].

The identification of charged hadrons relies on the specific ionization energy loss per unit length (dE/dx) in the TPC and on the information from the system of Ring Imaging Cherenkov (RICH) counters. The latter consists of two independent detectors, the Barrel and the Forward RICH, together covering over 90% of the full solid angle. Each of the RICH detectors contains two radiators of different refractive indices, allowing particle identification in the momentum range between 0.7 and 25 GeV/c. In the present analysis the HADSIGN tagging routine was used [5]. The algorithm provides charged kaon identification with efficiencies between 80% and 45%, and corresponding purities between 60% and 85%, depending on the particle momentum and the quality of the track reconstruction.

Simulated W^+W^- events were generated with the PYTHIA 5.7 generator [8]. The fragmentation model incorporated in the simulation was tuned to the DELPHI data measured at LEP1 [9].

3 Determination of $|V_{cs}|$ from the hadronic branching ratio of the W

In the leading order approximation, the cross-section for off-shell W^+W^- production in e^+e^- collisions is [10,11]:

$$\sigma(s) = \int_0^s ds_1 \int_0^{(\sqrt{s}-\sqrt{s_1})^2} ds_2 \; \rho(s_1)\; \rho(s_2)\; \sigma_0(s, s_1, s_2) \; , \tag{1}$$

where $\sqrt{s}$ is the total centre-of-mass (c.m.) energy and $\sqrt{s_1}$ and $\sqrt{s_2}$ are the masses of the two W bosons. The Breit-Wigner terms $\rho(s)$ describe the propagation and the coupling of the two W bosons to their decay products:

$$\rho(s_{1,2}) = \frac{1}{\pi}\,\frac{\Gamma_W}{M_W}\,\frac{s_{1,2}}{(s_{1,2}-M_W^2)^2 + s_{1,2}^2\Gamma_W^2/M_W^2} \; , \tag{2}$$

where M_W is the nominal W mass. The cross-section σ_0 can be written in terms of the ν, γ and Z exchange contributions and their interferences [10]. $|V_{cs}|$ enters the cross-section through the total width Γ_W of the W boson:

$$\Gamma_W(k) = k\Gamma_{c\bar{s}} + \sum_{i \neq c\bar{s}} \Gamma_i \; ,$$

where i runs over all $W^{\pm}$ decay modes apart from the $c\overline{s}$ channel and k is the ratio between $|V_{cs}|^2$ and the nominal value $|V_{cs}|_0^2 = 0.9493 \pm 0.0008$ determined from the CKM unitarity constraint [3]. The $|V_{cs}|$ dependence of the total cross-section (1) can be factorized as

$$\sigma(s,k) = \sigma(s,k=1)\ \frac{\Gamma_W^2(k)}{\Gamma_W^2(k=1)}\ f(k)\ ,$$

where $\sigma(s,k=1)$ is the total cross-section calculated for $k=1$. The correction factor $f(k)$ (Fig. 1a) comes from the widths Γ_W in the $W^{\pm}$ propagators (Eq. 2). Consequently, the value of $|V_{cs}|$ also affects decays other than $W^+ \to c\overline{s}$.

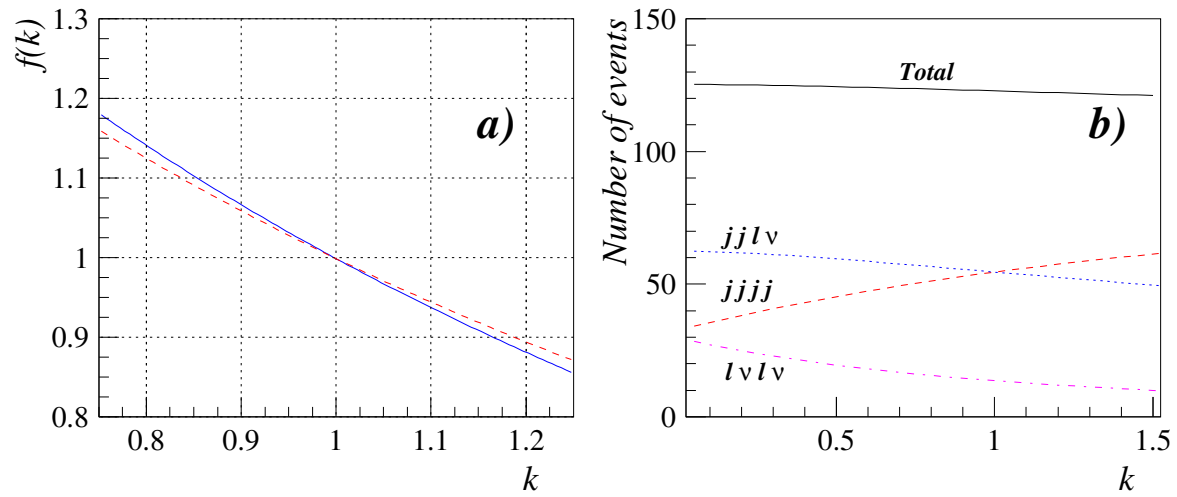

Figure 1: a) Correction factor to the $e^+e^- \to W^+W^-$ cross-section coming from the $|V_{cs}|$-dependent widths Γ_W in the $W^{\pm}$ propagators as a function of the ratio $k = |V_{cs}|^2/|V_{cs}|_0^2$. The solid curve shows the correction for the c.m. energy of 172 GeV and the dashed curve the correction for 161 GeV. b) Expected numbers of fully hadronic, mixed and fully leptonic decays of W pairs as a function of k. The numbers correspond to an integrated luminosity of approximately 10 pb^{-1} at 172 GeV c.m. energy and were evaluated in the leading-order approximation.

The ratio of the rate of fully hadronic ($jjjj$) decays of W pairs to that of fully leptonic ($l\nu l\nu$) and mixed ($jjl\nu$) decays (where one W decays hadronically and the other leptonically) is sensitive to $|V_{cs}|$ while the total number of produced W pairs is, to a very good approximation, insensitive to the change of $|V_{cs}|$, i.e. to the total W width (Fig. 1b). Note that this is true also beyond the leading order approximation (1), since the most important higher order corrections, e.g. corrections due to initial state radiation and Coulomb interaction, depend only very weakly on Γ_W. In extracting $|V_{cs}|$, the information from the total cross-section can therefore be neglected, and only the measured hadronic branching ratio of the W bosons need be used.

Using the data collected with the DELPHI detector at e^+e^- c.m. energies of 161 GeV and 172 GeV, corresponding to integrated luminosities of 9.93 pb^{-1} and 9.98 pb^{-1} respectively, DELPHI has obtained [12]:

$$BR(W \to hadrons) = 0.660^{+0.036}_{-0.037}(stat) \pm 0.009(syst)\ .$$

Assuming other parameters of the Standard Model, i.e. elements $|V_{ud}|$, $|V_{us}|$, $|V_{ub}|$, $|V_{cd}|$ and $|V_{cb}|$ of the CKM matrix, lepton couplings to W bosons, and the strong coupling

constant α_S, to be fixed at the values given in [3], this result implies

$$|V_{cs}| = 0.90 \pm 0.17(stat) \pm 0.04(syst) \ . \tag{3}$$

The systematic error on $|V_{cs}|$ includes a contribution due to uncertainties in the other parameters of the Standard Model (see Table 1).

4 Determination of $|V_{cs}|$ from flavour-tagged hadronic jets

Additional information about the value of $|V_{cs}|$ can be obtained by tagging the flavours of hadronic jets arising from fragmentation of the primary quarks from the $W^{\pm}$ decays. Compared to the extraction of $|V_{cs}|$ from the hadronic branching ratio of the W boson, its determination from the flavour-tagged hadronic jets relies neither on assumptions about the W-lepton couplings nor on the value of α_S. The following describes the selection of W^+W^--enhanced samples for this analysis, the subsequent flavour tagging of the hadronic jets, and the results obtained.

4.1 Selection of WW events containing hadronic jets

In an event, charged particles were selected with a polar angle between 10° and 170° and with a momentum between 0.4 GeV/c and the beam momentum. The lengths of the reconstructed tracks had to be larger than 15 cm, their impact parameters, both longitudinal and transverse with respect to the beam axis, had to be below 4 cm, and the maximum allowed uncertainty on the momentum measurement was 100%. Neutral particles were accepted if they deposited more than 0.5 GeV energy in the electromagnetic or hadronic calorimeters. For each event, all selected particles were clustered into jets using the LUCLUS algorithm [8] with a maximum separation, d_{ij}, of 6.5 GeV$^2/c^2$.

Requirements during the preselection of the events were very mild so that they did not reject any W pair decays but they rejected some of the background, e.g. a large number of $\gamma\gamma$ events. Three event classes were considered: fully hadronic decays where both W^+ and W^- decayed into quarks, mixed decays where one of the two gauge bosons decayed into an electron or a muon and a neutrino, and mixed decays with a tau lepton and a tau neutrino.

In the preselection of $W^+W^- \to q_1\overline{q}_2q_3\overline{q}_4$ candidates, events with more than seven charged tracks, at least three reconstructed hadronic jets and the sum of transverse momenta of measured particles, $\sum_i |p_{T,i}|$, larger than one third of the beam momentum were considered. Particles were then forced into a four-jet configuration and, in order to improve the momentum and energy resolution, a kinematically constrained fit was performed [12], imposing momentum conservation and the nominal $W^{\pm}$ mass to di-jet combinations. Of the three possible pairings of the four jets, that which minimized the χ^2 of the fit was chosen.

In the preselection of $W^+W^- \to q_1\overline{q}_2e^-(\mu^-)\overline{\nu}_{e(\mu)}$ events, an isolated track of a highly energetic particle, i.e. a lepton candidate, was required. In particular, a lepton candidate was chosen by finding the particle with the smallest value of the ratio $(\sum_j |\vec{p}_j|)/|\vec{p}_i|$, where $\vec{p}_i$ is the momentum of the candidate and the sum runs over the momenta of all particles in a 20° cone around the candidate's direction. The remaining tracks were then forced into a two-jet topology with each of the jets containing at least three particles. The

minimum reconstructed momentum sum of charged particles in these events, $\sum_{i\in ch} |\vec{p}_i|$, was one sixth of the beam momentum.

Candidates for the tau lepton mixed decays were forced into configurations with three jets. In addition, at least one tau-jet candidate was required, defined as an isolated jet containing only one charged particle with momentum larger than 3 GeV/c. The minimum transverse momentum sum of all measured charged particles, $\sum_{i\in ch} |p_{T,i}|$, was one fifth of the beam momentum, and the multiplicity in a hadronic jet was at least four.

At this stage a single event could enter more than one of the three classes. After the preselections above, several kinematic properties of the events were combined in order to separate the W pair signals from the remaining background.

For the fully hadronic channel, the number of originally reconstructed jets (i.e. number of jets before forcing the event into the four-jet configuration), the energies and multiplicities of these jets, the probability for the kinematically constrained fit, the angle between the faster jets from each of the two chosen di-jets, and the effective c.m. energy after initial state radiation were used. The latter was estimated either from the energy of an isolated highly energetic photon, if such a photon was reconstructed in the detector, or by taking the photon direction to be parallel to the beam and assuming a two-jet topology for the rest of the event [13,14]. The discriminating power of these variables stems from the fact that the dominant background, coming from $q\overline{q}$ creation in e^+e^- collisions, is frequently accompanied by a photon radiated from the initial state, resulting in a smaller effective c.m. energy. Jets from W pair decays are also distributed more uniformly in space than jets from $q\overline{q}(\gamma)$ events, where two out of four reconstructed jets are expected to arise from fragmentation of gluons, radiated predominantly at small angles to the quark directions. At the same time, these gluon jets are on average less energetic than jets in hadronic W decays.

A similar set of variables was used to describe the shape of mixed W^+W^- decays: the probability for the kinematically constrained fit, the effective c.m. energy, the total multiplicity, the acoplanarity of the event, the transverse missing momentum, and the number of reconstructed jets and their angular distribution. In addition, for mixed decays with electrons and muons, the momentum spectrum of the lepton candidate, the angle between the lepton and the direction of the missing momentum, and the lepton isolation (defined by the energy deposited inside a 10° cone around the lepton direction) were used. Using DELPHI electron and muon identification capabilities, it was possible to improve the separation of mixed W pair decays from the background events. The isolation of τ-jet candidates was defined in terms of the energy of charged particles inside a 30° cone around the τ-candidate. An attempt was also made to distinguish τ-jet candidates from other hadronic jets and from candidates due to misassociated tracks by the number of tracks in the jet and, as in the case of electrons and muons, by the angle that they formed with the missing momentum direction.

The probability that a measured event with a given value of a particular variable originated from a W decay was then calculated from the distribution of the corresponding simulated variable. By multiplying probabilities from all the quantities listed in the previous paragraphs, for each of the three classes, single discriminating variables P_{4q}, $P_{2qe(\mu)\nu}$ and $P_{2q\tau\nu}$ were obtained. To avoid multiple counting, every event was put in the class with the largest value of the discriminating variable. Because the number of events was small, the two classes of mixed decay candidates were then merged into one common class. Figure 2 shows the measured probability distributions for fully hadronic and mixed decay events according to the separating variables, as well as the expected distributions from corresponding simulated W^+W^- decays and from the background.

For further analysis, only events on the right side of the arrows were used, in order to maximize the product of the selection efficiency and the purity of the selected samples.

4.2 Flavour tagging of hadronic jets

After the selection, flavour-tagging was applied to the jets. The tagging relies on information from the DELPHI vertex and tracking detectors and on charged particle identification with the RICH counters. In order to separate jets originating from primary quarks with different flavours, the following discriminating properties were used:

- c- and s-jets can be tagged by high momentum charged kaons detected in the system of DELPHI RICH counters. These kaons are very likely to contain a primary s-quark or an s-quark from a $c \to s$ decay. Figure 3a shows the expected spectra when the highest momentum particle is identified as a charged kaon in jets with c-, s-, u- and d-flavours. Similarly, if a fast particle in a hadronic jet is an identified pion it is an indication of a u- or d-jet (see Fig. 3b). In each jet, the momentum-dependent probability for a particular jet flavour was calculated by considering only the highest momentum identified particle in the jet. In addition, such a particle was required to be among the three particles with highest momentum in the jet. The charge of the identified particle was also used to distinguish quarks from anti-quarks of the same flavour.
  As a minor contribution to the flavour separation in hadronic jets, the momentum distributions of identified muons, neutral kaons and Λ-baryons were also used. Muons are a signature for the semileptonic decay of charm hadrons, while reconstructed neutral kaons and Λ-baryons serve as an indication of a primary s-quark.

- c-jets can also be separated from the s-, u- and d-jets by the lifetime tag that is based on the impact parameter distribution of particles assigned to a particular jet [5]. From this distribution, one can build a probability P_M for the hypothesis that all the particles in a jet originate from the primary vertex. Due to the finite lifetime and the larger mass of the c-quark, this probability is on average smaller for charm jets than for light-quark jets (see Fig. 4).

These flavour signatures were combined into probabilities $P(q)$ for each jet to originate from a c-, s-, u- or d-quark in the same way as in the event selection procedure.

The influence of the combinatorial background was reduced by exploiting the correlation between the direction of a jet in the W rest frame and the flavour of its primary quark. W^+ bosons produced in e^+e^- collisions are partly polarized along their momenta and W^- bosons are polarized in the opposite direction [15]. Therefore, because of the $V-A$ structure of the W decays, down-like quarks and anti-quarks, i.e. s, d, $\overline{s}$ and $\overline{d}$, tend to follow the direction of the parent W (Fig. 5a). Information on the charge of the parent W can then be used to help decide whether the down-like decay product was a quark (d or s) or an anti-quark ($\overline{d}$ or $\overline{s}$).

In four-jet events, the W charge was assigned by making use of the strong correlation between the direction of the W and its charge [15,16]. The momenta of positively charged gauge bosons point mainly into the hemisphere determined by the direction of the positron beam (Fig. 5b). In $q\overline{q}l\overline{\nu}$ decays, the charge of the W was determined by the charge of the lepton candidate from a leptonic W-decay. The correlations between the jet direction and the flavour of the primary quark were then incorporated into the probabilities $P(q)$. Note, however, that the polarization of the $W^{\pm}$ (Fig. 5a), and thus also the background rejection

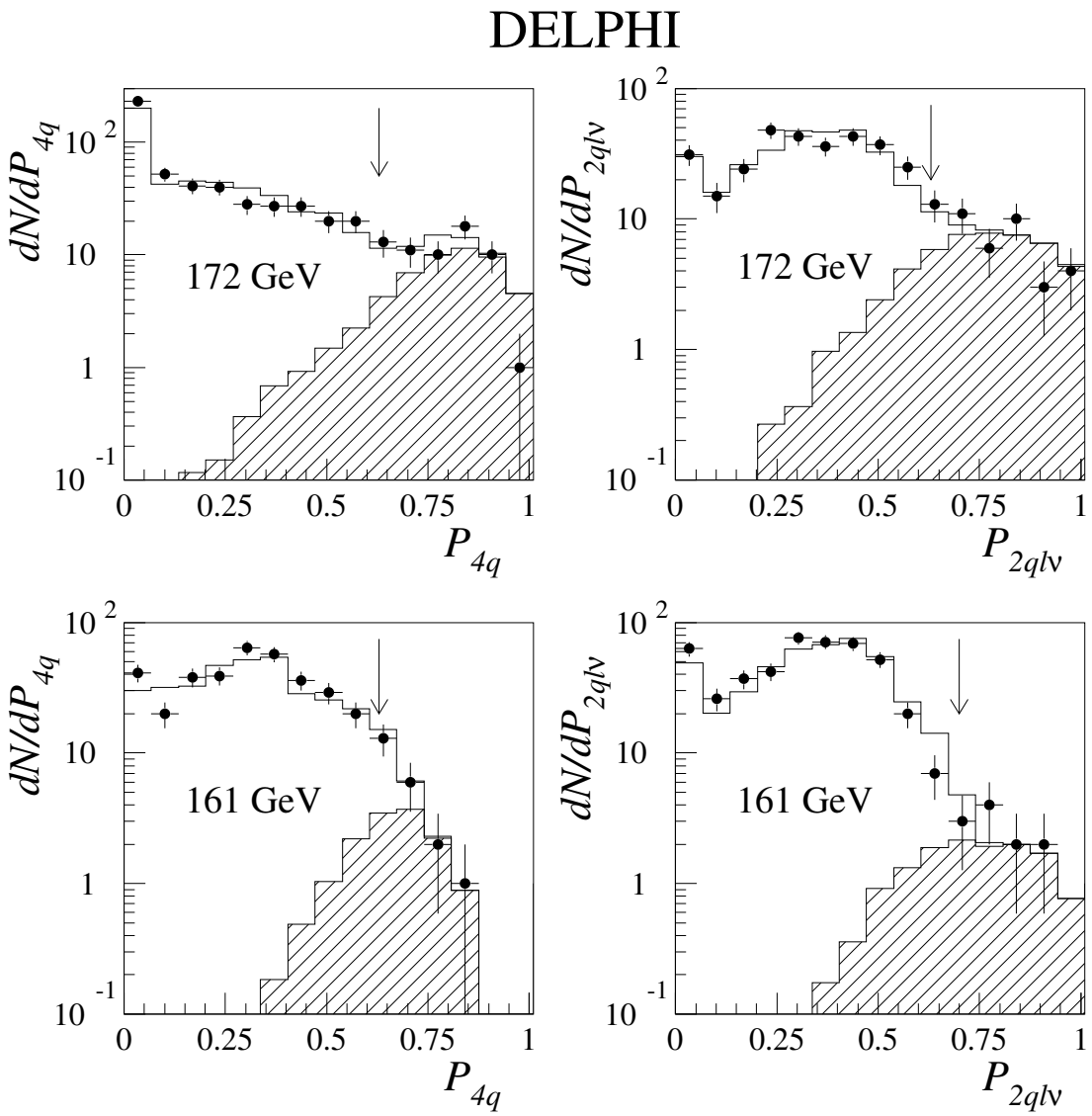

Figure 2: Distributions of the discriminating variables for preselected fully hadronic ($4q$) and mixed decay ($2ql\nu$) candidates. Measured spectra are displayed as points with error bars, expected signals as hatched histograms, and background as open histograms. The background is a sum of contributions from e^+e^- interactions giving $q\overline{q}(\gamma)$, $We\nu$, ZZ, Ze^+e^-, $e^+e^-\gamma$, Bhabha scattering and $\gamma\gamma$ collisions. The background in the mixed decay channel also contains fully leptonic decays of W pairs. For further analysis, only events to the right of the arrows were used.

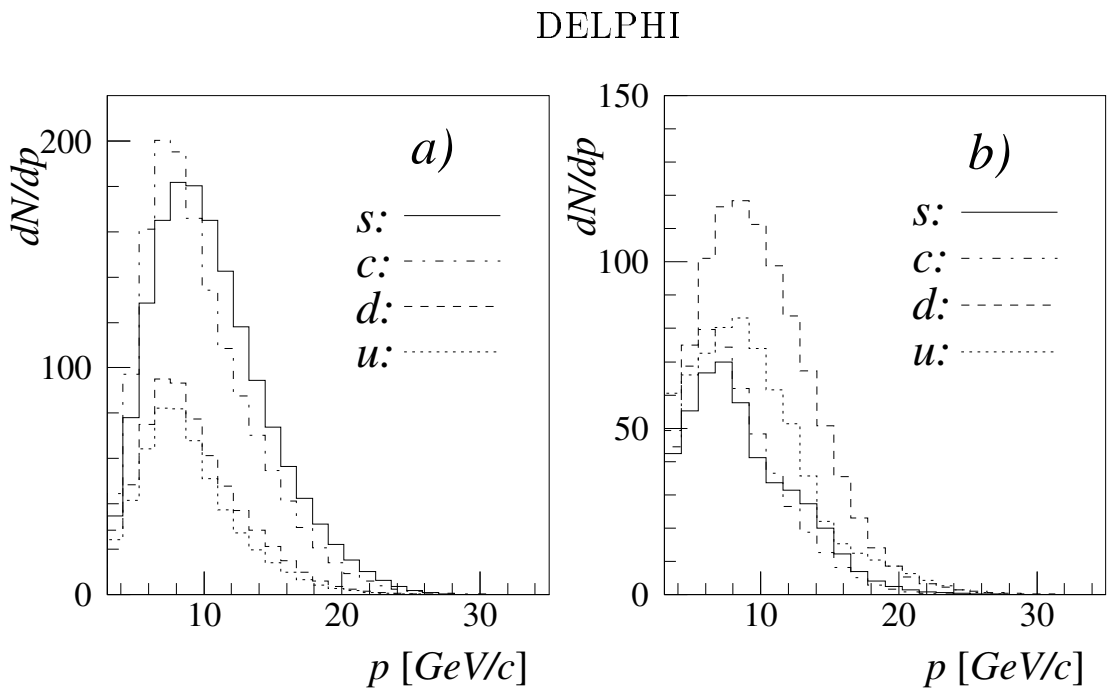

Figure 3: Momentum spectra of highest momentum particles in simulated c-, s-, u- and d-jets when the particles are identified as a) charged kaons or b) charged pions. The numbers of entries in the histograms correspond to approximately 15000 W^+W^- events generated with the nominal $|V_{cs}|_0$ value.

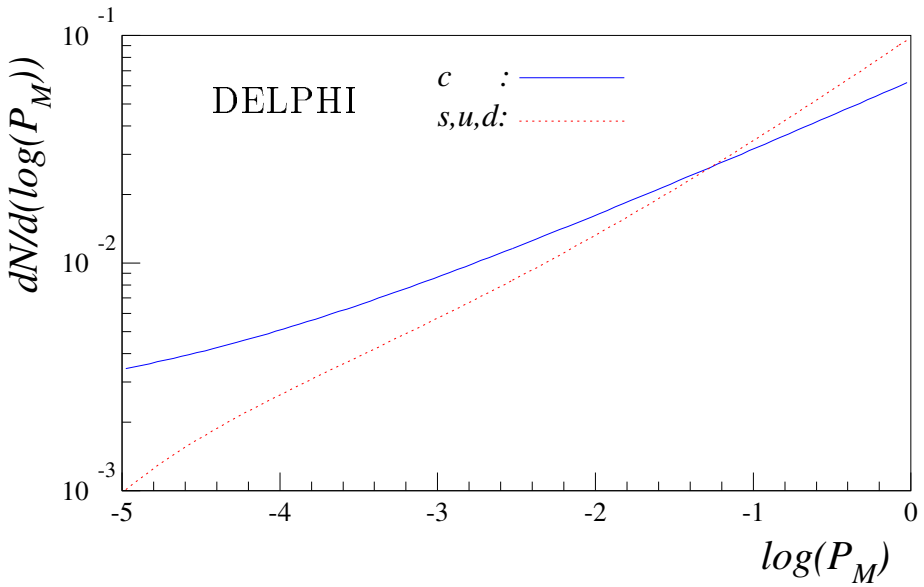

Figure 4: Simulated distributions of the probabilities P_M for the hypothesis that all charged particles in a jet come from the main vertex, for c-jets (full curve) and for s-, u- or d-jets (dotted curve).

power, will substantially increase with the increasing e^+e^- c.m. energy attainable in the coming years of LEP operation.

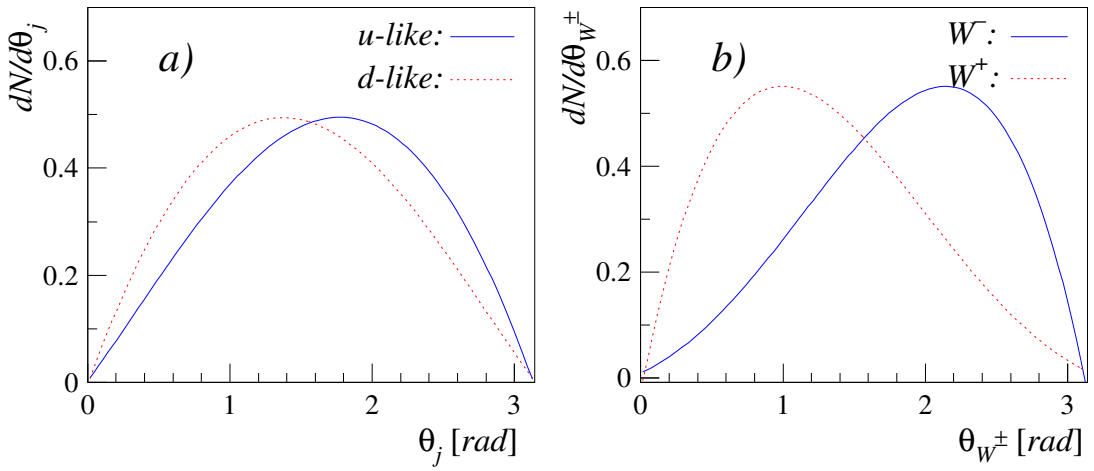

Figure 5: a) Simulated distribution of the angle between the momentum of the W and that of the corresponding jet from down-like (full curve) or up-like (dotted curve) quarks from W decays. b) Angular distributions of W^+ bosons (full curve) and of W^- bosons (dotted curve) with respect to the direction of the positron beam. The curves correspond to 172 GeV c.m. energy and include smearing of the $W^\pm$ direction due to reconstruction inefficiencies.

When combining the flavours of the two jets from hadronic $W^\pm$ decays, four different combinations were considered:

$$c\overline{s},\ \overline{c}s,\ u\overline{d},\ and\ \overline{u}d.$$

Decays into $u\overline{s}$, $s\overline{u}$, $c\overline{d}$, $d\overline{c}$, $c\overline{b}$, $b\overline{c}$, $u\overline{b}$ and $b\overline{u}$ pairs are strongly Cabibbo-suppressed; they were considered as a minor contribution to the $u\overline{d}$ and $\overline{u}d$ combinations (see below).

As the final separator, the probability, P_{cs}, that two jets come from the decay $W^+ \to c\overline{s}$ or $W^- \to \overline{c}s$ was constructed:

$$P_{cs} = \frac{P_1(c)P_2(\overline{s}) + P_2(c)P_1(\overline{s}) + P_1(\overline{c})P_2(s) + P_2(\overline{c})P_1(s)}{K_{nor}} ,$$

where K_{nor} is a normalization constant:

$$\begin{aligned} K_{\rm nor} &= P_1(c)P_2(\overline{s}) + P_2(c)P_1(\overline{s}) + P_1(\overline{c})P_2(s) + P_2(\overline{c})P_1(s) \\ &+ P_1(u)P_2(\overline{d}) + P_2(u)P_1(\overline{d}) + P_1(\overline{u})P_2(d) + P_2(\overline{u})P_1(d) , \end{aligned}$$

and indices 1 and 2 refer to the first and the second jets in di-jet combinations respectively. Figure 6 shows the P_{cs} distributions expected for $c\overline{s}$ and for $u\overline{d}$ di-jets from $W^\pm$ decays.

4.3 Results of the flavour tagging method

The value of $|V_{cs}|$ was extracted from the data by fitting the expected P_{cs} distributions to the spectra of the selected di-jet combinations by using the maximum likelihood method. The likelihood function

$$L = Mn(N; N_1, N_2, ..., N_i, ...; p_1, p_2, ..., p_i, ...)$$

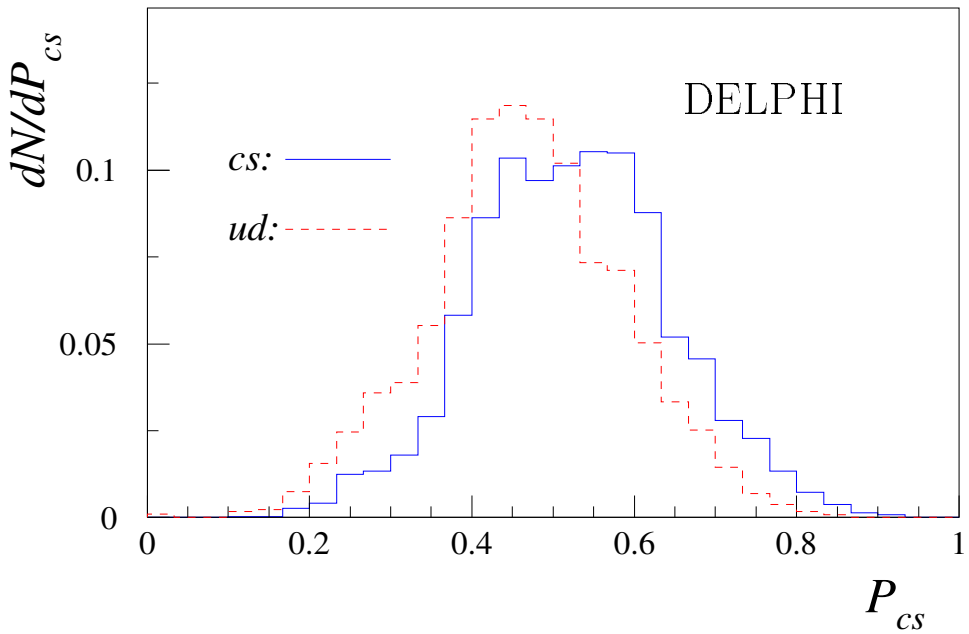

Figure 6: P_{cs} distributions for simulated $c\overline{s}$-jets (full histogram) and $u\overline{d}$-jets (dashed histogram).

was constructed as a multinomial probability [17] to observe N_1 out of N measured di-jets in the first bin of the P_{cs} distribution, N_2 in the second bin, etc. The probability p_i that a di-jet, randomly picked from the selected sample of WW candidates, would fall into the i-th bin depends on the value of $|V_{cs}|$ and was determined from the simulated signal and background samples.

The P_{cs} distributions extracted from the selected $jjjj$ and $jjl\overline{\nu}$ candidates were fitted simultaneously, with the migrations between the two channels taken into account. The fit was performed using the MINUIT program package [18].

Figure 7 shows the measured P_{cs} spectra together with fitted simulated distributions, while contributions to the overall P_{cs} spectrum are displayed in Fig. 8. The fraction of hadronic W^+ decays into $c\overline{s}$ quarks obtained was:

$$r^{(cs)} = \frac{\Gamma(W^+ \to c\overline{s})}{\Gamma(W^+ \to hadrons)} = 0.46^{+0.18}_{-0.14}(stat) \pm 0.07(syst) \ . \tag{4}$$

The fraction can be converted into the value of $|V_{cs}|$:

$$|V_{cs}| = 0.94^{+0.32}_{-0.26}(stat) \pm 0.13(syst). \tag{5}$$

The contributions to the overall systematic error are discussed in the next section.

Combining results (3) and (5) gives

$$|V_{cs}| = 0.91^{+0.15}_{-0.14}(stat) \pm 0.05(syst) \ . \tag{6}$$

Unitarity of the CKM matrix, incorporated in the framework of the Standard Model, is experimentally supported by very stringent limits on the first order flavour-changing neutral currents [3]. Therefore assuming unitarity but allowing for more than three quark generations further constrains the upper-bound errors on the value (6) of $|V_{cs}|$:

$$|V_{cs}| = 0.91 \ ^{+0.065}_{-0.15} \ , \tag{7}$$

where the errors incorporate both statistical and systematic uncertainties.

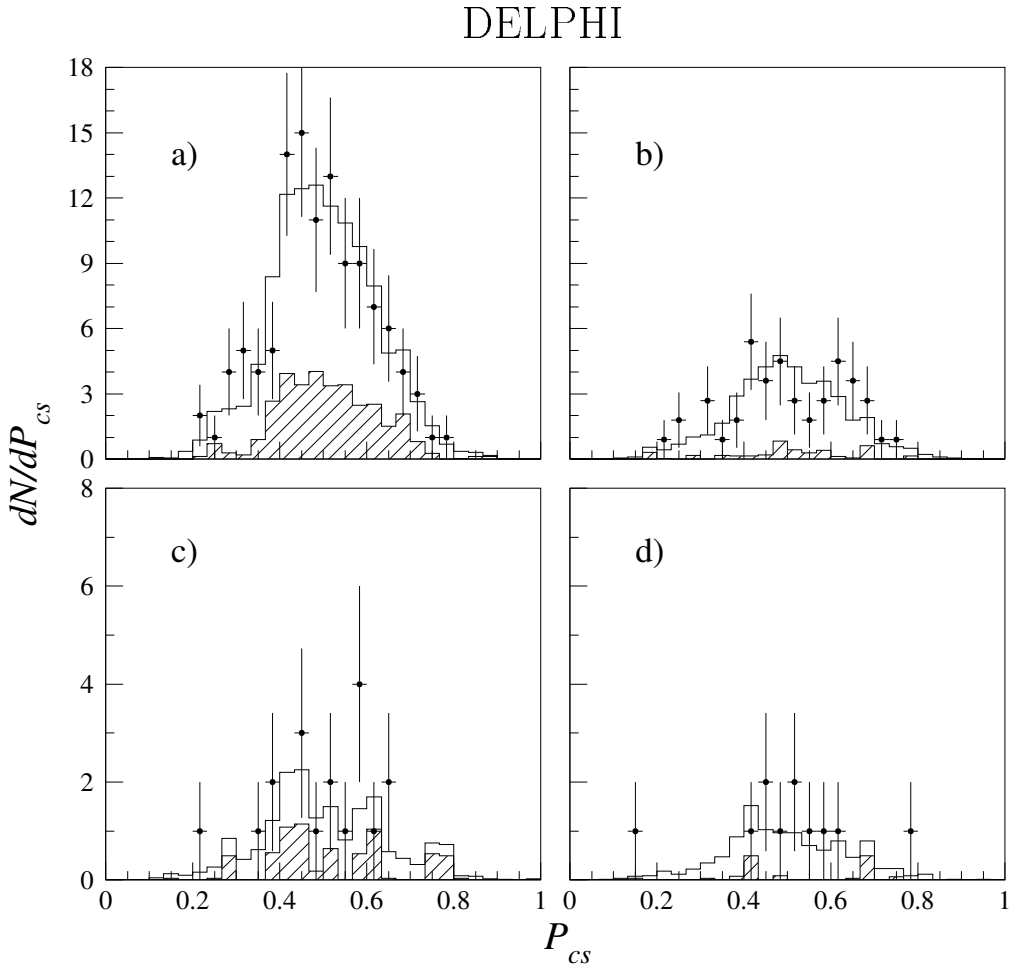

Figure 7: Measured P_{cs} spectra (points with error bars) together with the best fit simulated predictions (open histograms) for $jjjj$ decays (a) and (c) and for $jjl\overline{\nu}$ events (b) and (d). Hatched histograms correspond to the background contribution. Data shown in Figs. a) and b) were taken at 172 GeV c.m. energy while data in c) and d) were collected at 161 GeV.

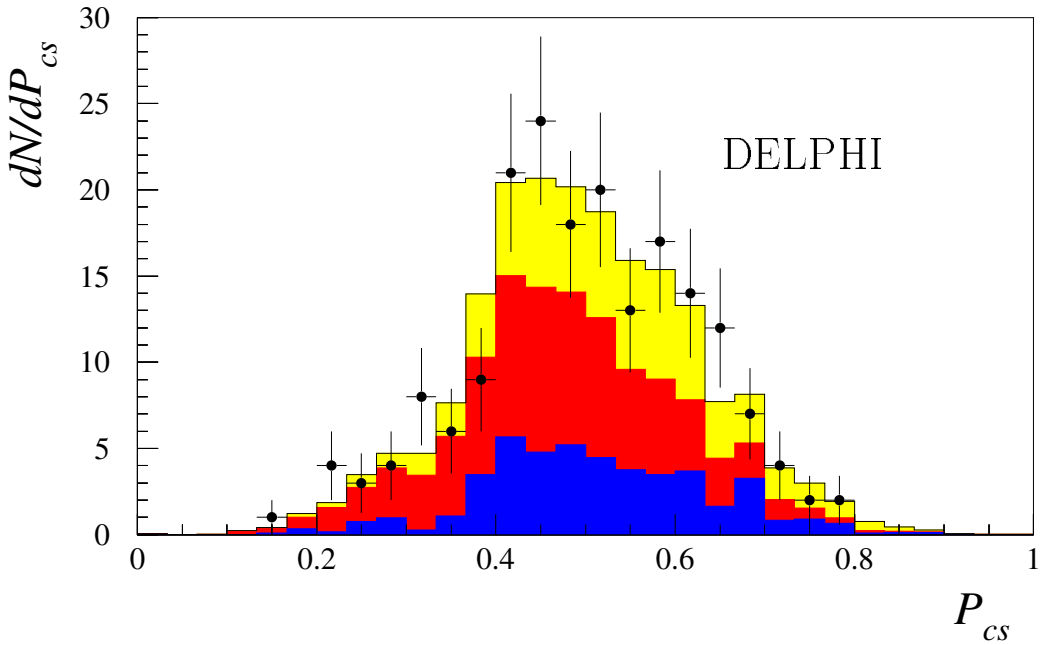

Figure 8: The sum of the $jjjj$ and the $jjl\overline{\nu}$ P_{cs} spectra. The measured distribution is shown by the points with error bars and the best fit by the histogram. The shaded areas show fractions of particular contributions: $W^+ \to c\overline{s}$ (light shading), $W^+ \to u\overline{d}$ together with the Cabibbo-suppressed decays (medium shading), and the background (dark shading).

5 Systematic uncertainties on $|V_{cs}|$

The systematic uncertainties on $|V_{cs}|$ extracted from the measured hadronic branching ratio of the $W^{\pm}$ [12] are dominated by the uncertainties on the background normalization for the fully hadronic W^+W^- decays, and by the uncertainty in the efficiency calculation (see Table 1). Apart from the Feynman diagrams involving W pairs (the so-called "CC03 diagrams" [16], containing s-channel γ and Z exchange and t-channel ν exchange), there are also other electroweak diagrams, involving either zero, one or two massive vector bosons, which can lead to the same final state fermions. The effects of the interference between the CC03 diagrams and the additional diagrams were estimated by using the four-fermion generator EXCALIBUR [19] and have been treated as additional correction factors to the absolute normalization [12,13] of the expected signal. The possible uncertainties on these values were added to the overall systematic error on the measurement (Table 1). In addition, the contributions due to the uncertainties on the value of $|V_{cd}|$ and on the strong coupling constant $\alpha_S(M_{W^{\pm}})$ [3] were also considered. They were found to be small (Table 1), while the impact of uncertainties in other parameters of the Standard Model is negligible.

The systematic error on $|V_{cs}|$ as measured by tagging the flavour of hadronic jets from W decays is determined mainly by the precision of tuning the representation of the DELPHI tracking detectors in simulated events [20]. The systematic uncertainty due to the lifetime tag was estimated using Z^0 hadronic decays collected during the short runs at the Z^0 pole in 1996. Samples with different fractions of $b\overline{b}$, $c\overline{c}$ and light-quark decays were selected by cutting at different values of the probability P_M that all charged tracks in one hemisphere came from the primary vertex (see section 4.2). Measured and simulated P_M

Table 1: The contributions to the systematic uncertainties on the measurement of $|V_{cs}|$ for the two methods and for the combined result. Note that for the first method the error due to the finite Monte Carlo (MC) sample is included in the error coming from the efficiency calculation.

	Systematic error on $\|V_{cs}\|$ from		
Source of uncertainty	BR($W \to q\overline{q}$)	Flavour tag	Combined
Efficiency calculation	± 0.027	-	± 0.019
Background normalization	± 0.028	± 0.029	± 0.028
"CC03"-correction factors	± 0.015	< 0.001	$^{+0.010}_{-0.011}$
$\|V_{cd}\|$	± 0.004	< 0.001	± 0.003
α_S	± 0.001	< 0.001	± 0.001
Lifetime tag	-	± 0.100	$^{+0.029}_{-0.025}$
$K^{\pm}$,$\pi^{\pm}$ spectra	-	± 0.058	$^{+0.017}_{-0.016}$
MC statistics	-	± 0.040	± 0.012
Total	± 0.042	± 0.126	$^{+0.050}_{-0.048}$

distributions in the opposite hemisphere were then compared and simulated distributions for jets of particular flavours were corrected in order to reproduce the measured ones. The same corrections were applied to the simulated P_M distributions of jets in W^+W^- decays and background processes used for determination of $|V_{cs}|$ from flavour-tagged hadronic jets. The results (4-5) were obtained with the corrected simulated samples and differ from those obtained with the uncorrected simulated spectra by approximately 15%. The uncertainty of the correction due to the finite number of recorded Z^0 events is quoted as a contribution to the systematic uncertainty of our measurement (Table 1). In the future, the uncertainty can be reduced if longer periods of running at the Z^0 centre-of-mass are interspersed with the LEP high energy runs.

The tuning of the parameters of the fragmentation model used for event simulation was checked with samples of particles collected at the Z^0 pole and during high energy runs in 1996, as well as with the large number of Z^0 decays collected during the operation of LEP1. As for the estimation of the lifetime tag systematic uncertainties, c-, s-, or u/d-enhanced samples were selected by cutting at different values of P_M and by requiring identified fast kaons or pions in one hemisphere. The momentum spectra of fast kaons and pions in the other hemisphere were then compared to the appropriate simulated distributions. Following the same procedure as for the lifetime tagging method, the contribution to the overall systematic uncertainty was determined to be ± 0.058.

6 Conclusion

The sample of approximately 100 W pairs collected by the DELPHI detector in 1996 has been used to measure the value of the $|V_{cs}|$ element of the CKM matrix. The value

extracted from the measured hadronic branching ratio of the W boson was

$$|V_{cs}| = 0.90 \pm 0.17(stat) \pm 0.04(syst) \ ,$$

while tagging the flavour of jets from W-decays gave

$$|V_{cs}| = 0.94^{+0.32}_{-0.26}(stat) \pm 0.13(syst) \ .$$

The precision of the two values combined,

$$|V_{cs}| = 0.91^{+0.15}_{-0.14}(stat) \pm 0.05(syst) \ ,$$

already surpasses the precision of the combination of all previous measurements [21–24]. Moreover, unlike the previous measurements which are limited by uncertainties from the theoretical input, the uncertainty on this result is dominated by the statistical error. By the end of LEP2 data-taking it can therefore be expected that the precision will be substantially improved.

Acknowledgements

We are greatly indebted to our technical collaborators, to the members of the CERN-SL Division for the excellent performance of the LEP collider, and to the funding agencies for their support in building and operating the DELPHI detector.
We acknowledge in particular the support of
Austrian Federal Ministry of Science and Traffics, GZ 616.364/2-III/2a/98,
FNRS–FWO, Belgium,
FINEP, CNPq, CAPES, FUJB and FAPERJ, Brazil,
Czech Ministry of Industry and Trade, GA CR 202/96/0450 and GA AVCR A1010521,
Danish Natural Research Council,
Commission of the European Communities (DG XII),
Direction des Sciences de la Matière, CEA, France,
Bundesministerium für Bildung, Wissenschaft, Forschung und Technologie, Germany,
General Secretariat for Research and Technology, Greece,
National Science Foundation (NWO) and Foundation for Research on Matter (FOM), The Netherlands,
Norwegian Research Council,
State Committee for Scientific Research, Poland, 2P03B06015, 2P03B03311 and SPUB/P03/178/98,
JNICT–Junta Nacional de Investigação Científica e Tecnológica, Portugal,
Vedecka grantova agentura MS SR, Slovakia, Nr. 95/5195/134,
Ministry of Science and Technology of the Republic of Slovenia,
CICYT, Spain, AEN96–1661 and AEN96-1681,
The Swedish Natural Science Research Council,
Particle Physics and Astronomy Research Council, UK,
Department of Energy, USA, DE–FG02–94ER40817.

References

[1] N. Cabibbo, Phys. Rev. Lett. **10** (1963) 531.
[2] M. Kobayashi, T. Maskawa, Progr. Theor. Phys. **49** (1973) 652.
[3] Particle Data Group, Review of Particle Physics, Phys. Rev. **D54** (1996) 1.
[4] DELPHI Collaboration, P. Aarnio et al., Nucl. Instr. Meth. **A303** (1991) 233.
[5] DELPHI Collaboration, P. Abreu et al., Nucl. Instr. Meth. **A378**, (1996) 57.
[6] P. Chochula et al., *The DELPHI Silicon Tracker at LEP2*, CERN-PPE/97-155.
[7] A.C. Benvenuti et al., *The DELPHI Small Angle Tile Calorimeter*, contribution to IEEE NSS 1994, IEEE Trans. Nucl. Sci. **42** (4) (1995) 478.
[8] T. Sjöstrand, *PYTHIA 5.7 / JETSET 7.4*, CERN-TH.7112/93 (1993).
[9] DELPHI Collaboration, P. Abreu et al., Z. Phys. **C73** (1996) 11.
[10] T. Muta, R. Najima and S. Wakaizumi, Mod. Phys. Lett. **A1** (1986) 203.
[11] A. Ballestrero et al., *Determination of the Mass of the W Boson*, Physics at LEP2, eds. G. Altarelli, T. Sjöstrand and F. Zwirner, CERN 96-01 (1996) Vol. 1, p. 141.
[12] DELPHI Collaboration, P. Abreu et al., E. Phys. J. **C2** (1998) 581.
[13] DELPHI Collaboration, P. Abreu et al., Phys. Lett. **B397** (1997) 158.
[14] P. Abreu, D. Fassouliotis, A. Grefrath, R.P. Henriques and L. Vitale, *SPRIME, A Package for Estimating the Effective* $\sqrt{s'}$ *Centre of Mass Energy in* $q\overline{q}(\gamma)$ *Events*, DELPHI Note 96-124 PHYS 632.
[15] Z. Ajaltouni et al., *Triple Gauge Boson Couplings*, Physics at LEP2, eds. G. Altarelli, T. Sjöstrand and F. Zwirner, CERN 96-01 (1996) Vol. 1, p. 525.
[16] W. Beenakker, F.A. Berends et al., *WW cross section and distributions*, Physics at LEP2, eds. G. Altarelli, T. Sjöstrand and F. Zwirner, CERN 96-01 (1996) Vol. 1, p. 79.
[17] W.T. Eadie, D. Drijard, F.E. James, M. Roos, B. Sadoulet, *Statistical Methods in Experimental Physics*, North-Holland (1971).
[18] F. James, *MINUIT Function Minimisation and Error Analysis*, CERN Program Library Long Writeup D506.
[19] F.A. Berends, R. Kleiss, R. Pittau et al., *EXCALIBUR*, Physics at LEP2, eds. G. Altarelli, T. Sjöstrand and F. Zwirner, CERN 96-01 (1996) Vol. 2, p. 23.
[20] G. Borisov, C. Mariotti, Nucl. Instr. Meth. **A372** (1996) 181.
[21] H. Abramowicz et al., Z. Phys. **C15** (1982) 19.
[22] CLEO Collaboration, A. Bean et al., Phys. Lett. **B317** (1993) 647.
[23] Mark III Collaboration, Z. Bai et al., Phys. Rev. Lett. **66** (1991) 1011;
Mark III Collaboration, J. Adler et al., Phys. Rev. Lett. **62** (1989) 1821.
[24] E691 Collaboration, J.R. Raab et al., Phys. Rev. **D37** (1988) 2391.